Electronic Supplementary Material (ESI) for Physical Chemistry Chemical Physics.

Supporting Information

for

Ultra-high permeable phenine nanotube membranes for water desalination

Supriyo Naskar[1], Anil Kumar Sahoo[1,2,3], Mohd Moid[1], and Prabal K. Maiti[1,†]

[1]Center for Condensed Matter Theory, Department of Physics, Indian Institute of Science, Bangalore 560012, India

[2] Max Planck Institute of Colloids and Interfaces, Am Mühlenberg 1, 14476 Potsdam, Germany

[3] Fachbereich Physik, Freie Universität Berlin, Arnimallee 14, 14195 Berlin, Germany

[†]Corresponding author, e-mail: maiti@iisc.ac.in

Table of Contents

1. Details of the simulated systems

Table S1. Details of the (12,12) PNT(H) system in water.

System	Initial box dimensions	Total number of atoms
(12,12) PNT(H)	63.12 × 62.92 × 98.26	31390

Table S2. Details of the systems for PMF Calculation of ions along the nanotube axis. The PMF profile plotted in the figure 2 of the main text is performed on the following systems. The chirality of each nanotube is (9,9).

System	Initial box dimensions	Total number of atoms
Na^+ along the CNT	58.9 × 59.1 × 98.2	27770
K^+ along the CNT	58.9 × 59.1 × 98.2	27770
Cl^- along the CNT	58.9 × 59.1 × 98.2	27770
Water along the CNT	58.9 × 59.1 × 98.2	27774
Na^+ along the PNT(H)	58.9 × 59.1 × 98.2	27788
K^+ along the PNT(H)	58.9 × 59.1 × 98.2	27785
Cl^- along the PNT(H)	58.9 × 59.1 × 98.2	27788
Water along the PNT(H)	58.9 × 59.1 × 98.2	27789
Na^+ along the PNT	58.9 × 59.1 × 98.2	27788

Table S3. Details of the systems for the calculation of spontaneous ion insertion inside nanotubes. The ion number profile as a function of simulation time, plotted in the figure S4 of the SI is performed on the following systems. The chirality of each nanotube is (9,9).

System	Number of Na^+	Number of Cl^-	Number of water molecules	Total number of atoms
CNT with 150mM NaCl solution	26	26	8942	27670
CNT with 150mM KCl solution	26	26	8942	27670
CNT with 600mM NaCl solution	101	101	8808	27418
CNT with 600mM KCl solution	101	101	8832	27490
PNT(H) with 150mM NaCl solution	26	26	8955	27685
PNT(H) with 150mM KCl solution	26	26	8955	27685
PNT(H) with 600mM NaCl solution	102	102	8827	27453
PNT(H) with 600mM KCl solution	102	102	8836	27480

Table S4. Details of the PNT membrane system. The water flow calculation is performed on the following systems. The chirality of each nanotube is (9,9).

System	Number of Na^+	Number of Cl^-	Number of water molecules	Total number of atoms
PNT in 600 mM NaCl solution	53	53	4593	24829
PNT(H) in 600 mM NaCl solution	44	44	3852	20860

Table S5. Details of the systems for osmosis study. The chirality of each nanotube is (9,9).

System	Salinity of the system	Number of Na^+	Number of Cl^-	Number of water molecules	Total number of atoms
PNT	600 mM NaCl solution	51	51	9612	50826
	1000 mM NaCl solution	85	85	9544	50690
	2000 mM NaCl solution	170	170	9374	50350
PNT(H)	600 mM NaCl solution	50	50	9334	46534
	1000 mM NaCl solution	84	84	9266	46398
	2000 mM NaCl solution	168	168	9098	46062

2. Validation of the partial atomic charges and force-field

In order to validate the parametrized partial charges and force field for PNT, we simulate the (12,12) PNT(H) of length 50 Å in pure water for 500 ns. The final structure after 500 ns simulation is very much comparable to the original experimental crystal structure (Figure S2). We then calculate the root mean square deviation (RMSD) of the MD simulated PNT(H) with respect to the crystal structure. For the RMSD calculation, we choose the carbon atoms only and choose part of the PNT which is of the same length as in the crystal structure (~ 17.1 Å). The calculated RMSD shows very small fluctuation (~0.4 Å), which confirms that the partial atomic charges and the force field parameters are accurate enough to maintain the crystal structure of PNT (Figure S2). Furthermore, it is well known from the literature that CNT of chirality (12,12) with a diameter of 16.27 Å contains bulk-like water structure inside and allows passage of almost all kinds of salt ions, without any energy barrier[1]. Likewise, one would expect that PNT of chirality (12,12) will not be an appropriate nanomaterial for the water filtration process. Thus, for the water desalination application, we choose PNT of chirality (9,9) which has been synthesized experimentally[2] and has a much smaller diameter (d=12.21 Å) than (12,12) PNT. All the results presented in this main text are for (9,9) PNT.

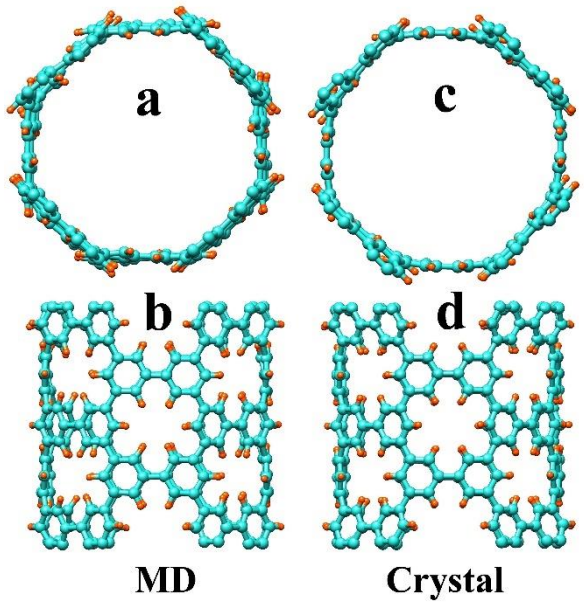

Figure S1. *Validation of the molecular model of PNT. (a) Top view and (b) side view of the MD simulated structure of PNT(H) after 500 ns. (c) Top view and (d) the side view of the experimentally synthesized crystal structure. The experimental crystal structure is obtained from Cambridge Crystallographic Database Centre (CCDC-1844346)[28]. Cyan represents carbon atoms and red represents hydrogen atoms.*

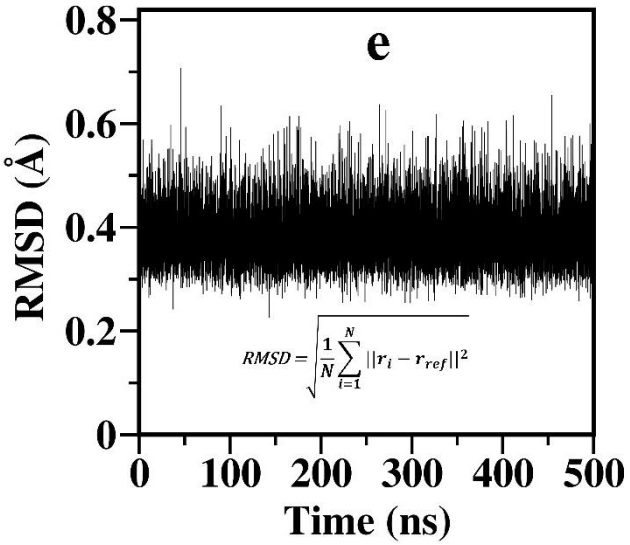

Figure S2. *Root-mean-square deviation. Time evolution of the root-mean-square deviation (RMSD) in atomic positions of the in silico modeled PNT with respect to the crystal structure.*

3. Density and distribution of water in the vicinity of the nanotube

The structure and dynamics of water inside a nanopore and in its vicinity play a crucial role in determining both water permeation and salt rejection properties of the nanopore. We, therefore, probe the water density and the electrostatics around and inside the nanotube. To calculate these properties for each system (PNT, PNT(H), and CNT) as shown in Figure 1 of main text, we use the last 25 ns data from the 100 ns-long simulation during which only the nanotube's central segment is restrained such that the dynamics of the terminal functional groups remain unaffected. The average water densities along the nanotube's axial and radial directions are plotted in Figure S3a and S3b, respectively. Unlike CNT, we observe periodic spikes in the density of water along the axial direction of PNT. This signifies that some positions inside PNT are favorable for water. From a careful examination of the trajectory, we find that water molecules are more in number in the vicinity of the hydrogen atoms attached to the phenine group. As the hydrophobicity of CNT wall is reduced with defects[3,4], we observe more water near the periodic defects of PNT. Around the two terminal regions, the number of waters inside PNT is fewer than that of PNT(H), which is due to the presence of bulky t-Bu groups. Furthermore, from the radial density profiles, one can discern the more ordered structure of water inside CNT compared to that of PNT. Also, owing to the periodic defects in the PNT wall—where water molecules stick—the hydrophobic nature of PNT is expected to be much lesser than CNT (with a smoother wall). As a result, a greater number of water molecules are found inside PNT compared to CNT (Figure S4 of SI). Additionally, due to the negative electrostatic potential of the PNT nanotube we found a greater number of Na^+ ion inside the PNT compared to the CNT (Figure S3 (c)). For both nanotubes, we found no Cl^- ion enters the nanotube during the simulation time (Figure S3 (d)). Owing to the negative potential energy of the PNT, we found the number density of Cl^- is slightly lower in PNT near the vicinity of the nanotube compared to CNT (Figure S3 (d)).

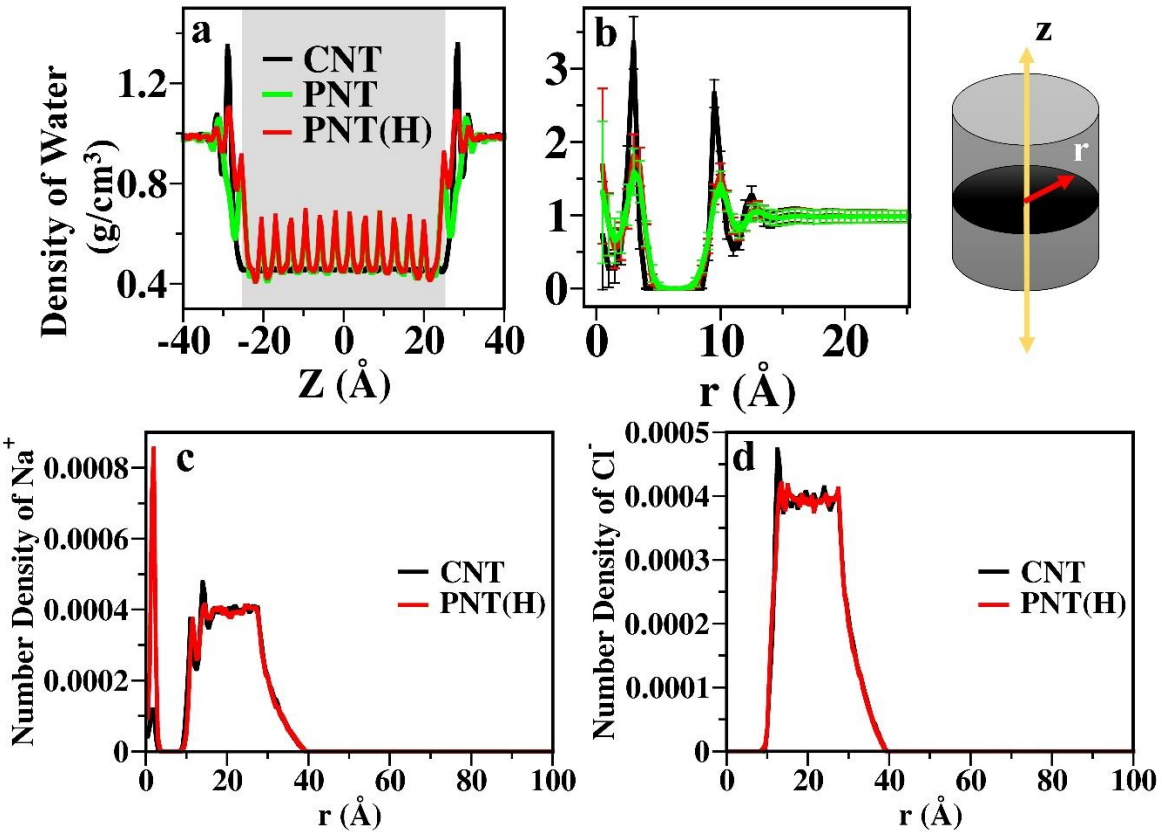

Figure S3. *(a) Water density along the axis of the nanotube. The shaded area in the graph corresponds to the region inside the nanotube. (b) Water density along the radial direction of the nanotube. In the inset of the graph the direction Z and r is shown. (c) Number density of* Na^+ *ion along the radial direction of the nanotube. (d) Number density of* Cl^- *ion along the radial direction of the nanotube.*

4. Number of ions and water molecules inside different nanotubes

We have simulated a single (9,9) CNT/PNT(H) inside a water box with NaCl salinity 150mM and 600mM. We then calculated the number of ions entering into the nanotube during the 100 ns long simulation.

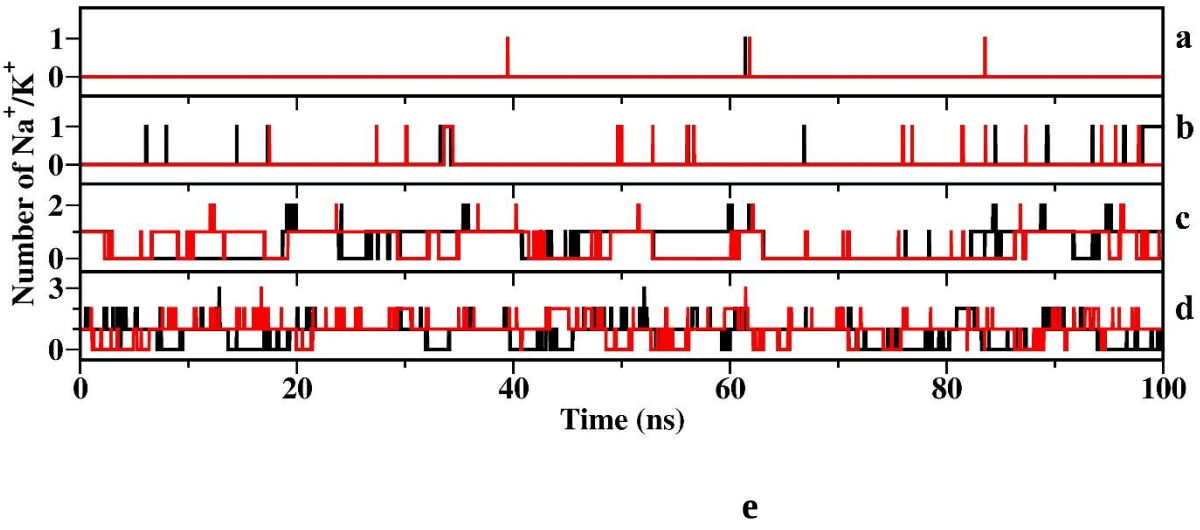

e

Figure S4. *Numbers of ions inside the nanotube during the simulation. The Red line corresponds to the number of* Na^+ *ion where the system contains only NaCl salt and the black line corresponds to the number of* K^+ *ion where the system contains only KCl salt. Each system contains either (a) and (b) a single PNT or (c) and (d) a single CNT. The chirality of each nanotube is (9,9). The salinity of each system is (a) 150 mM (b) 600 mM (c) 150 mM and (d) 600 mM. (e) Number of water molecules inside different (9,9) nanotubes.*

5. Radial distribution function and coordination number of ions in bulk and confinement

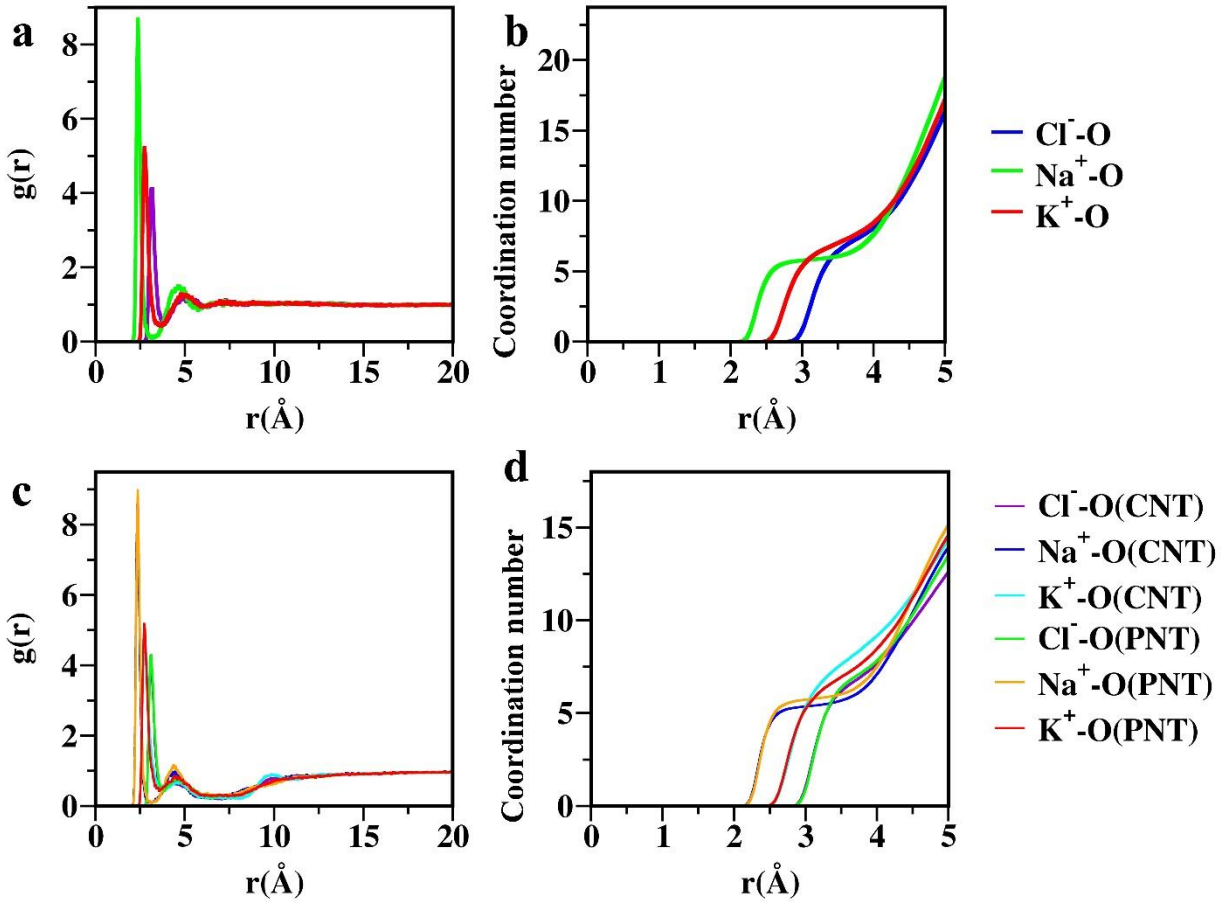

Figure S5. *(a) Radial distribution function and (b) coordination number of different ions in bulk with the oxygen atoms of water. (c) Radial distribution function and (d) coordination number of different ions inside the nanotube with the oxygen atoms of water.*

6. Water flux and salt rejection data

Table S6. Water flux and salt rejection values across the PNT membrane.

Pressure (MPa)	**Water Flux (/ns/tube)**	**Na^+ Flux (/ns/tube)**	**Cl^- Flux (/ns/tube)**	**Na^+ Rejection (%)**	**Cl^- Rejection (%)**
5	0.12 ± 0.003	0.000 ± 0.000	0.000 ± 0.000	100	100
50	2.21 ± 0.01	0.000 ± 0.000	0.000 ± 0.000	100	100
100	4.30 ± 0.02	0.004 ± 0.000	0.000 ± 0.000	90.76	100
200	9.00 ± 0.01	0.006 ± 0.000	0.000 ± 0.000	94.30	100
300	15.43 ± 0.01	0.033 ± 0.000	0.000 ± 0.000	81.46	100
400	20.50 ± 0.03	0.057 ± 0.000	0.006 ± 0.000	75.62	99.72

Table S7. Water flux and salt rejection values across the PNT membrane scaled by the membrane area.

Pressure (MPa)	**Water Flux (/ns/tube/Å^2)**	**Na^+ Flux (/ns/tube/Å^2)**	**Cl^- Flux (/ns/tube/Å^2)**	**Na^+ Rejection (%)**	**Cl^- Rejection (%)**
5	5.5×10^{-5} ± 0.00	0.000 ± 0.000	0.000 ± 0.000	100	100
50	0.00095 ± 0.00	0.000 ± 0.000	0.000 ± 0.000	100	100
100	0.00184 ± 0.00	2×10^{-6} ± 0.000	0.000 ± 0.000	90.76	100
200	0.00385 ± 0.00	2.5×10^{-6} ± 0.000	0.000 ± 0.000	94.30	100
300	0.0066 ± 0.00	1.4×10^{-5} ± 0.000	0.000 ± 0.000	81.46	100
400	0.00876 ± 0.00	2.5×10^{-7} ± 0.000	2.8×10^{-7} ± 0.000	75.62	99.72

Table S8. Water flux and salt rejection values across the PNT(H) membrane.

Pressure (MPa)	**Water Flux (/ns/tube)**	**Na^+ Flux (/ns/tube)**	**Cl^- Flux (/ns/tube)**	**Na^+ Rejection (%)**	**Cl^- Rejection (%)**
50	3.16 ± 0.02	0.012 ± 0.000	0.001 ± 0.000	66.67	97.36
50	28.13 ± 0.03	0.151 ± 0.000	0.027 ± 0.000	53.04	91.53
100	54.76 ± 0.02	0.400 ± 0.001	0.119 ± 0.001	36.05	80.90
200	110.14 ± 0.02	0.875 ± 0.001	0.324 ± 0.000	30.43	74.24
300	164.75 ± 0.04	1.524 ± 0.002	0.675 ± 0.001	19.04	64.14
400	223.14 ± 0.03	2.229 ± 0.001	1.065 ± 0.001	12.56	58.22

Table S9. Water flux and salt rejection values across the PNT(H) membrane scaled by the membrane area.

Pressure (MPa)	**Water Flux (/ns/tube/Å^2)**	**Na^+ Flux (/ns/tube/Å^2)**	**Cl^- Flux (/ns/tube/Å^2)**	**Na^+ Rejection (%)**	**Cl^- Rejection (%)**
50	0.00135 ± 0.00	5.1×10^{-6} ± 0.000	4.1×10^{-7} ± 0.000	66.67	97.36
50	0.01202 ± 0.00	6.4×10^{-5} ± 0.000	1.2×10^{-5} ± 0.000	53.04	91.53
100	0.0234 ± 0.00	0.00017 ± 0.000	5.1×10^{-5} ± 0.000	36.05	80.90
200	0.04707 ± 0.00	0.00037 ± 0.000	0.00014 ± 0.000	30.43	74.24
300	0.7041 ± 0.00	0.00065 ± 0.000	0.00029 ± 0.000	19.04	64.14
400	0.09536 ± 0.00	0.00095 ± 0.000	0.00046 ± 0.000	12.56	58.22

7. Collective diffusion model

We are able to reproduce the water permeation rate with increasing pressure using collective diffusion model originally developed by Zhu *et al.* [5].The movement of water inside a nanopore generally follow coupled many-body dynamics and is described by a collective co-ordinate $n(t)$, which denotes the net amount of water permeation at time t. In the stationary state where a net water flux (j_w) exists, the j_w can be written as

$$j_w = \frac{\langle n(t) \rangle}{t} \tag{S4}$$

In equilibrium, the average value of water permeation vanishes on the average, i.e., $\langle n(t) \rangle = 0$. However, due to thermal fluctuations, spontaneous transport of water occurs which can be captured through $n(t)$. It has been shown that when t is much longer than the velocity autocorrelation time of n, and the mean square of n, $\langle n^2(t) \rangle$, follows Einstein relation

$$\langle n^2(t) \rangle = 2D_n t \tag{S5}$$

where D_n is defined as the collective diffusion coefficient of n.

In the presence of a pressure gradient, ΔP, across the membrane, the water flow across it attains a steady-state value, and the configuration of the membrane reaches a stationary state. In such a stationary configuration, the water inside the channel is assumed to be very close to the equilibrium condition, provided that the pressure gradient is not very high. Then the equilibrium value of D_n can be used to define the biased random walk of n. The probability distribution of n at time t, $p(n,t)$, is described as a one-dimensional diffusion in a linear potential using the following Smoluchowski equation,

$$\frac{\partial p(n,t)}{\partial t} = D_n \left(\frac{\partial^2}{\partial n^2} + \beta f l \frac{\partial}{\partial n} \right) p(n,t) \tag{S6}$$

$$\Rightarrow p(n,t) = \frac{1}{\sqrt{4\pi D_n t}} \exp\left[-\frac{(n + D_n \beta f l t)^2}{4 D_n t}\right] \quad \text{(S7)}$$

where f is the force due to the pressure gradient, l is the length of the system across which the pressure gradient is applied, and $\beta = (K_B T)^{-1}$.

The average value of n can be calculated as,

$$\langle n(t) \rangle = \int_{-\infty}^{\infty} n(t)\, p(n,t)\, dn = \frac{f l}{K_B T} D_n t \quad \text{(S8)}$$

From equation (S4), the water flux then follows,

$$j_w = \frac{\langle n(t) \rangle}{t} = \frac{f l}{K_B T} D_n = -\frac{V \Delta P}{N K_B T} D_n \quad \text{(S9)}$$

Here $f l = -\frac{A l \Delta P}{N} = -\Delta P V / N$; $A =$ cross-sectional area of the membrane, $V = A \times l =$ volume of the simulation box, ΔP is the pressure gradient, $N =$ the total number of water molecules.

In order to calculate the collection diffusion coefficient D_n, we first evaluate the number of water permeation event, $n(t)$ at each time step from the equilibrium simulation. The time series of the permeation event has been plotted in figure S6 (a). Then MSD of n for each system is presented in figure S6 (b). From the slopes of the graph, the D_n values are determined to be 50.00 /ns and 549.1 /ns for systems PNT and PNT(H) membrane, respectively.

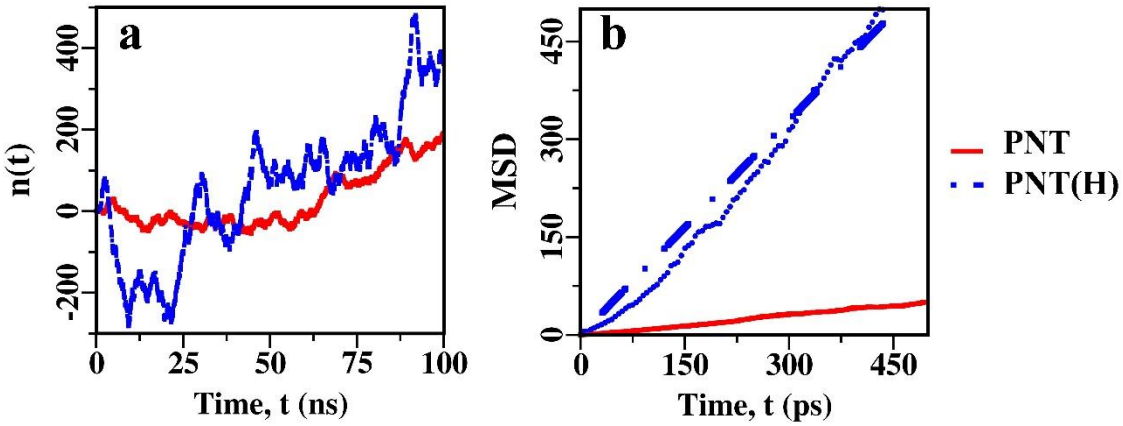

Figure S6. *(a) Time evolution of $n(t)$ for equilibrium MD simulation for two different types of PNT membrane. (b) Mean square displacement of $n(t)$. For each system, the trajectory n(t) is evenly divided into 200 short time periods. In each period, $n(t)$ is treated as an independent sub trajectory $n_i(t)$ and is shifted so that $n_i(t=0)=0$. The average over $n_i^2(t)$ is then defined as the MSD(t). From the best fit of the one half of the slope, the collection diffusion coefficient D_n is evaluated. A similar methodology has been implemented previously by Zhu et. al. in the original article of the collective diffusion model*[5] *(Phys. Rev. Lett.* ***2004,*** *93, (22), 224501).*

8. Osmotic permeability calculation

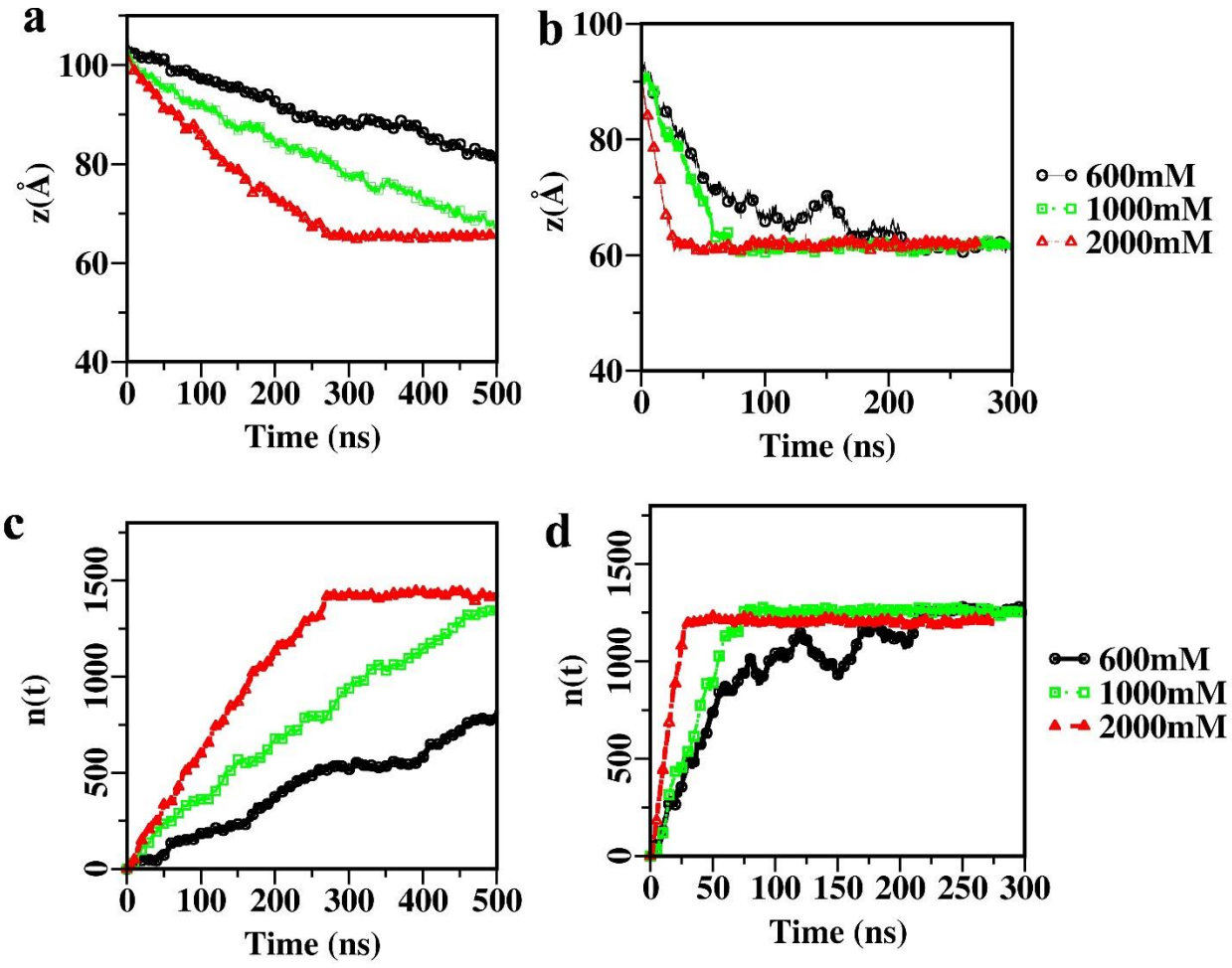

Figure S7. *Time evolution of inter-membrane distance and average water permeation rate. The center of mass distance between the two membranes in the osmosis simulation as a function of simulation time for (a) PNT and (b) PNT(H). Average water permeation per membrane as a function of simulation time for (c) PNT and (d) PNT(H).*

Table S10. Details of the trajectory interval in which osmotic permeability calculation was performed.

System	Salinity of the system	Trajectory interval in which osmotic permeability calculation was performed
PNT	600 mM NaCl solution	50 ns to 500 ns
	1000 mM NaCl solution	50 ns to 300 ns
	2000 mM NaCl solution	50 ns to 200 ns
PNT(H)	600 mM NaCl solution	5 ns to 100 ns
	1000 mM NaCl solution	5 ns to 50 ns
	2000 mM NaCl solution	5 ns to 20 ns

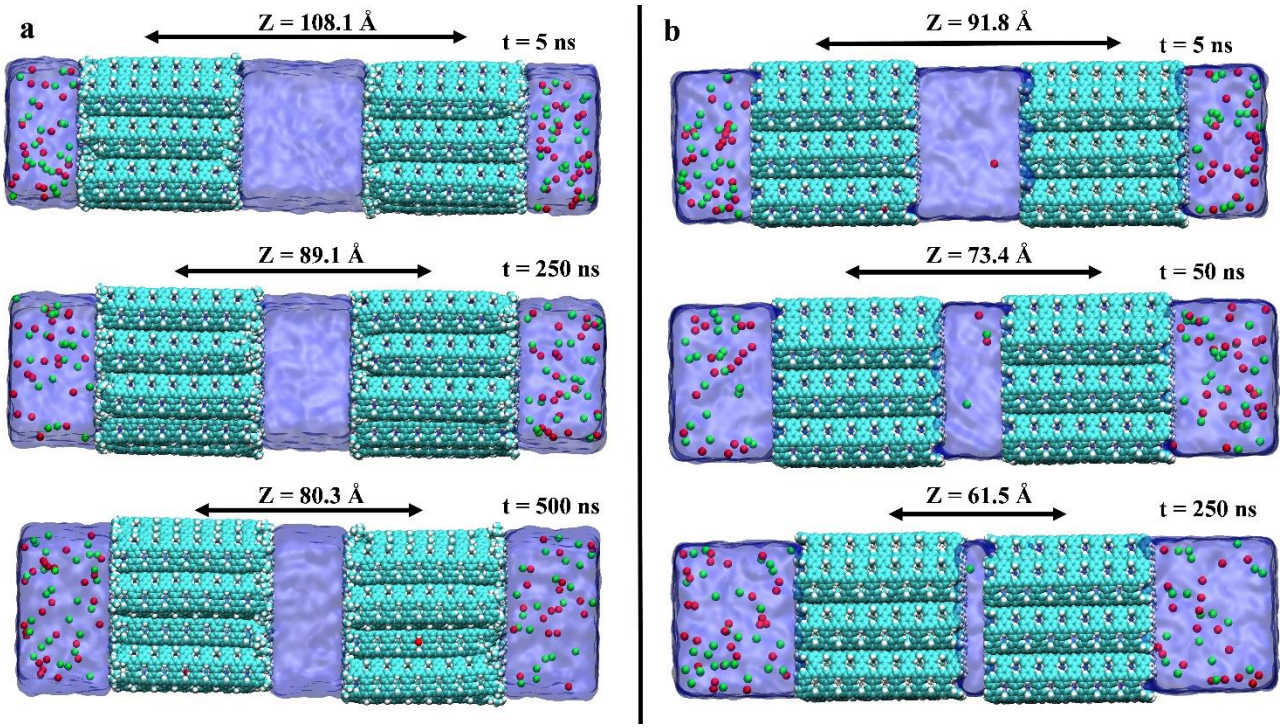

Figure S8. *Instantaneous snapshots of the osmotic system in the different time intervals for (a) PNT and (b) PNT(H) systems. Red dots are Na^+ ions and green dots are Cl^- ions. The blue shade is the water box. The cyan color represents the PNT or PNT(H) membranes.*

9. Comparison of water permeation and salt rejection of PNT and CNT

In order to compare the water permeation and salt rejection of PNT and CNT, we have performed few calculations on the CNT. In particular, we performed equilibrium and non-equilibrium simulation of CNT having chirality (9,9). We performed simulation the (9,9) CNT membrane in three pressure gradient 50 MPa, 200 MPa, 400 MPa to have direct comparison with the PNT. All the CNTs have hydrogen as the end-functionalization group. The flux values obtained for (9,9) CNT from the non-equilibrium simulation and the collective diffusion model is given in the below table,

Table S11. Details of water permeation and salt rejection of PNT and CNT.

Systems	PNT		PNT(H)		CNT(Simulation)		CNT (Theory)
Pressure Gradient	Water Flux(/ns/tube)	Salt Rejection (%)	Water Flux(/ns/tube)	Salt Rejection (%)	Water Flux(/ns/tube)	Salt Rejection (%)	Water Flux(/ns/tube)
50MPa	2.21	100	28.13	72.3	46.1	89.6	54.3
200MPa	9.0	97.2	110.14	52.3	198.6	27.7	217.1
400MPa	20.5	87.7	223.14	35.4	419.4	11.8	434.2

The collective diffusion model accurately predicts the flux data over a wide range of pressures, signifying the robustness of the model. We find that the water flux of (9,9) CNT is higher than that of the (9,9) PNT(H). The latter can be explained by comparing the free energy profiles (PMFs) for water transport through CNT and PNT (see Fig. 2 in the manuscript). The PMF of water is very smooth for CNT, whereas it is rugged for PNT. So, water gets trapped transiently in local minima, which reduces the permeability of PNT(H) compared to CNT of the same chirality.

10. A note on PMF calculation

The PMF reported in the manuscript is for single PNT as shown using schematic representation in figure 1.

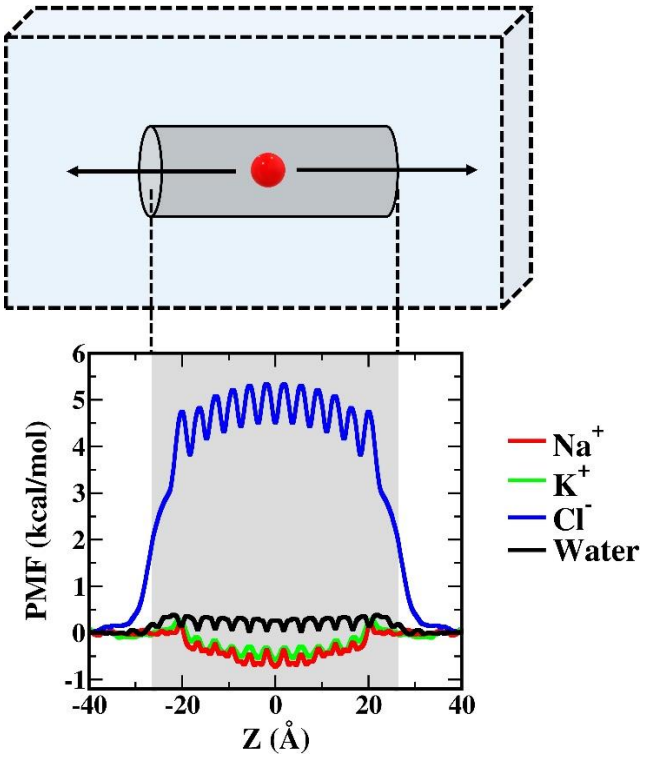

Figure S9. Simulation setup for PMF calculation. A single PNT/CNT was placed in a water box. Then ions were moved along the axis of the PNT using umbrella potentials. PMF was constructed using WHAM method.

Conformations of the end tertiary butyl groups are different when there are neighboring PNTs to interact as in a PNT membrane. See Figure-2 to better understand the dynamics of headgroups after 100 ns simulation for a single PNT and a PNT membrane. The tertiary butyl groups of a single PNT protrude out and do not block the pore entrances. In contrary, the tertiary butyl groups of the PNT membranes interact with each other and reduce the effective pore sizes of the PNTs. As a result, ions experience a larger barrier in a PNT membrane compared to a single PNT.

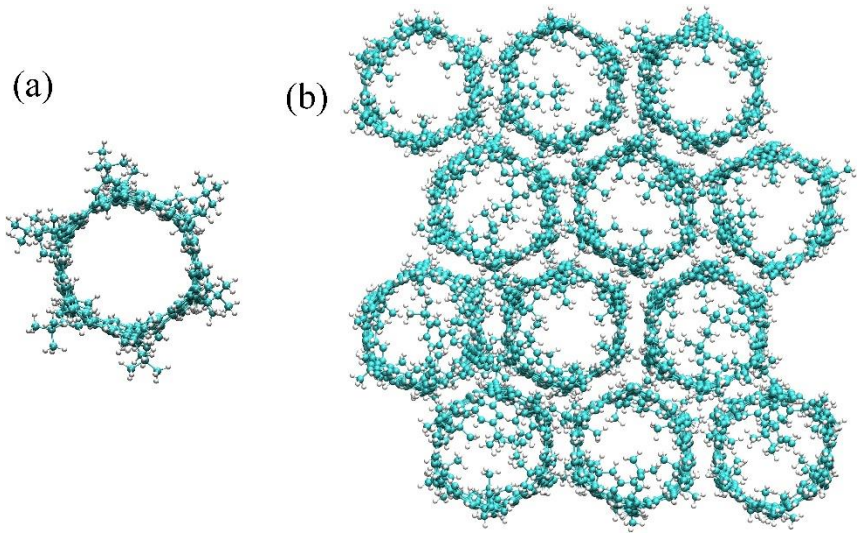

Figure S10. (a) Structure of a single PNT immersed in water after 100 ns of simulation. (b) Structure of a PNT membrane immersed in water after 100 ns of simulation. Water and ions are not shown for clarity.

References

1 J. A. Thomas and A. J. H. McGaughey, Water flow in carbon nanotubes: Transition to subcontinuum transport, *Physical Review Letters*, 2009, **102**, 1–4.

2 Z. Sun, K. Ikemoto, T. M. Fukunaga, T. Koretsune, R. Arita, S. Sato and H. Isobe, Finite phenine nanotubes with periodic vacancy defects, *Science*, 2019, **363**, 151–155.

3 S. Marbach and L. Bocquet, Osmosis, from molecular insights to large-scale applications, *Chemical Society Reviews*, 2019, **48**, 3102–3144.

4 T. Z. X. Hong, L. You, M. Dahanayaka, A. W.-K. Law and K. Zhou, Influence of Substitutional Defects in ZIF-8 Membranes on Reverse Osmosis Desalination: A Molecular Dynamics Study, *Molecules,* , DOI:10.3390/molecules26113392.

5 F. Zhu, E. Tajkhorshid and K. Schulten, Collective diffusion model for water permeation through microscopic channels, *Physical Review Letters*, 2004, **93**, 1–4.